Highly efficient remote controlled release system based on light-driven DNA nanomachine functionalized mesoporous silica

Yongqiang Wen,*[a] Liping Xu,[a] Wenqian Wang,[a] Danyang Wang,[a] Hongwu Du,[a] Xueji Zhang*[a, b]

[a] *Research Center for Bioengineering & Sensing Technology, University of Science and Technology Beijing, Beijing 100083, China, Email: wyq_wen@iccas.ac.cn*

[b] *Department of Chemistry, University of South Florida, 4202 E. Fowler Ave. CHE-205A, Tampa, Fl 33620-5250, USA. E-mail: xzhang@cas.usf. edu; Fax: (+1) 941-3712534*

Materials and methods

1. Materials

Boric acid, acetic acid, ethylenediamine-tetraacetic acid, NaCl, $MgCl_2.6H_2O$, StainsAll®, formamide, tris(hydroxymethyl)-aminomethane (Tris), and ethidium bromide, bis(*p*-sulfo natophenyl) phenylphosphine dihydrate dipotassium salt were purchased from Aldrich. 5-ethylthiotetrazole, controlled pore glass (CPG) and reagents for automated DNA syntheses were purchased from Glen research. The phosphoramidite monomer bearing an azobenzene group was synthesized according to reported method.[S1, S2] Microcon® size-exclusion centrifugal filter devices were purchased from Millipore. Citrate coated AuNPs were made in-house according to the literatures (Handley, 1989). Tetraethoxysilane (TEOS, 28%), n-cetyltrimethylammonium bromide (CTAB, ≥99%), ammonium hydroxide solution (25%), 1-ethyl-3-(3-dimethylaminopropyl) carbodiimide (EDC, 99%), N-Hydroxysuccinimide (NHS, 98%), 3-Aminopropyltriethoxy-silane (APTES, 99%), succinic anhydride (99%), sodium citrate tribasic dihydrate, tannic acid, and Rhodamine B were purchased from Sigma Company. Hydrogen tetrachloroaurate (Ⅲ) was purchased from Jinke reagent company, China. All buffers were prepared with ultra-pure MilliQ water (resistance > 18 MΩ cm^{-1}).

2. Methods

Standard automated oligonucleotide solid-phase synthesis was performed on an Applied Biosystems 394 DNA synthesizer. UV-Vis spectra were measured on a Varian Cary 300 biospectrophotometer. High-performance liquid chromatography (HPLC) was performed using a Techcomp LC2000 series HPLC. Gel electrophoresis experiments were carried out on an

acrylamide 20 × 20 cm vertical DYCZ24 electrophoresis unit, and an agarose 8.5 × 8 cm horizontal DYCZ31 separation minigel system. Scanning electron microscope (SEM) was performed with a JEOL-6700FE instrument. All fluorescence spectra were recorded on a Hitachi F-4500 FL Spectrophotometer in PBS buffer. Transmission electron microscopy (TEM) images were obtained using a Philips CM 200 kV electron microscope. Powder X-ray diffraction (XRD) patterns were collected using a Rigaku D/max 2500 equipped with Cu Kα radiation. Fourier transform infrared (FT-IR) spectra were taken on a Bruker-EQUINOX55 spectrometer. N_2 adsorption-desorption isotherms were obtained at 77 K on a Micromeritics ASAP2020 automated sorption analyzer. The BET model was applied to evaluate the specific surface areas. Pore size and pore volume were determined from the adsorption data by BJH method. X-ray photoelectron spectroscopy (XPS) data were obtained with an ESCALab220i-XL electron spectrometer from VG Scientific using 300 W Al Kα radiation. The base pressure was about 3×10^{-9} mbar. The binding energies were referenced to the C_{1s} line at 284.6 eV from adventitious carbon.

3. Synthesis of oligonucleotides

The oligonucleotides were constructed on CPG supports using conventional phosphoramidite chemistry. For the sequences modified by one or more azobenzene groups in the interior of the DNA sequence, azobenzene groups was incorporated using a modified protocol in which the coupling and deprotection times were extended to eight and two minutes, respectively. Products were cleaved from the support by treatment with concentrated NH_4OH for 16 h at 55°C. The NH_4OH solution was decanted and dried down to yield the crude DNA mixture. The crude mixture obtained was purified by preparative reverse-phase HPLC with 0.03 M triethylammonium acetate (TEAA), pH 7 and a 1%/min gradient of 95% CH_3CN/5% 0.03 M TEAA at a flow rate of 1 mL/min. Quantification was estimated based on UV-Vis absorbance at 260 nm.

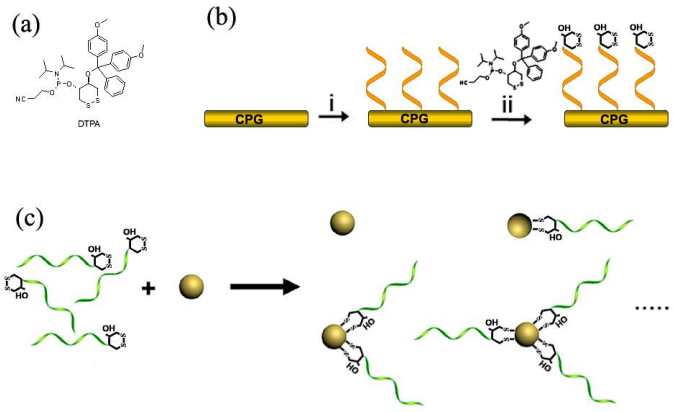

Fig. S1. (a) The structure of molecule DTPA. (b) DTPA was grafted on the DNA sequence during the DNA synthesise process. (c) DTPA-modified DNA were conjugated to AuNPs.

DNA sequences (Azo represents azobenzene; DTPA represent the cyclic disulfide-containing phosphate derivative, which can form two Au-S bond linkages with the surface of AuNPs (Supplementary Information); underlined bases represent stem moieties). **a**: 5'-(Rhodamine green)-CCTAGCAACAGACCGCACTTTATGATAGCAA (Azo)GC(Azo) TA(Azo)GG-Dabcyl-3'; **b**:5'-(H_2NC_6)CCTAGCAACAGACCGCACTTTATGATAGCAA(Azo)GC(Azo)TA(Azo)GG-(DTPA)-3'.

4. Preparation and characterization of the AuNPs and AuNP-DNA monoconjuagtes

Gold colloids with mean diameters of about 4.0 nm were synthesized by the citrate/tannic acid method.[S3] The citrate-stabilized gold colloids were subsequently exchanged with a negatively charged phosphine shell using bis(p-sulfonatophenyl)- phenyl-phosphine dehydrate dipotassium salt. DNA-AuNP monoconjugates were prepared by mixing AuNPs with the cyclic disulfide-modified ssDNA **b** in 1:1 molar ratio and incubated for 12 h in PBS buffer (20 mM, 50 mM NaCl, pH 7.2). The method used for isolating DNA-AuNP monoconjugates, AuNP dimer and trimer from the reaction mixture is gel electrophoresis (2.5 % agarose gel at 5 V/cm, 10 mM PBS buffer), followed by recovery of the appropriate band. Collected fractions were concentrated in Microcon 50000 MWCO centrifugal filters, which could be further attached onto the MS particles to create the controlled release system through a coupling reaction with carboxyl-end-capped MS.

5. Preparation and characterization of the controlled release system

The functionalization procedure of MS was shown in Fig. 1c. To investigate the photoinduced

controlled release property of the MS-DNA-AuNPs system in aqueous solution, rhodamine B (RhB) was used as a model guest molecule to diffusion-filled into the pores of the MS by immersing the MS-DNA-AuNPs particles in a 0.15 M solution for 6 h at 60°C, which is higher than the melting temperature of the DNA nanomachine (Fig. S2). At that temperature, the DNA nanomachine takes an extended structure, allowing the guest molecules to get into the openings of the pores favorably. The temperature was then reduced to room temperature so that the AuNPs were capped to the openings of pores on the MS particles in the PBS buffer. The surface-adsorbed dye, uncapped dye in the holes, and excessive AuNPs were washed with PBS buffer and removed by repeated washing and centrifugation.

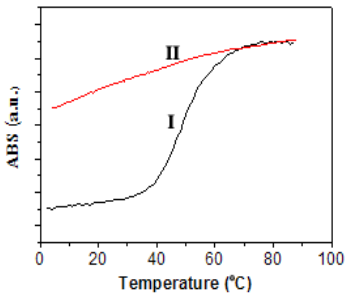

Fig. S2. Typical melting temperature curves of the DNA sequence when the incorporated Azo were at trans (curve I) and cis form (curve II). The data was obtained by monitoring the changes in absorbance at 260 nm with temperatures.

6. Photo-controlled release experiments

Azobenzene compounds are typical materials displaying a reversible photoisomerization effect: UV irradiation causes a trans-to-cis isomerization, and exposure to visible light causes the reverse configurational transition, which could lead to the stability changes of DNA duplex bearing azobenzene groups on a D-threoninol linker.[S1,S4] To demonstrate the effect of the nanomachine, the DNA nanomachine-modified MS system was placed at the bottom of a cuvette in Tris-HCl buffer and irradiated by a xenon lamp (500 W) using filters centered at λ = 365 nm for UV light and centered at λ = 450 nm for visible light. The amount of rhodamine B (RhB) released was determined by detection of the intensity changes of fluorescence at 570 nm.

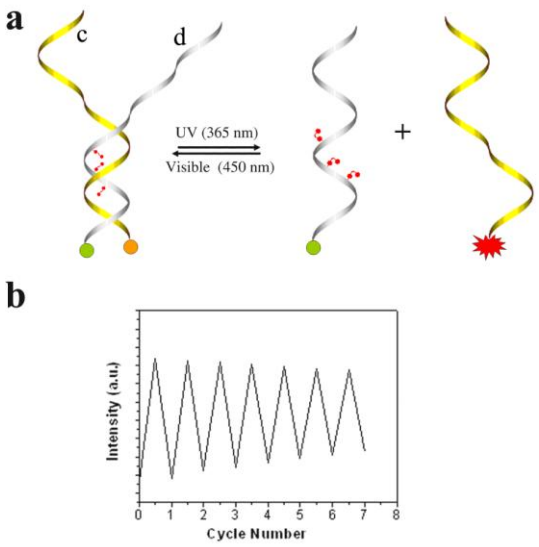

Fig. S3. (a) Schematic of the working principle of the bimolecular DNA (sequence **c:** 5'-(Rhodamine green)-CCTAGCAACAGACCGCACTTCA-3'; sequence d: 5'-GCACTTTAT GATAGCAA(Azo)GC(Azo)TA(Azo)GG-Dabcyl-3') nanoswitch under the irradiation of visible (high FRET) and UV light (low FRET). (b) Fluorescence intensity conversation showed the reversibility of the DNA nanoswitch, indicating the operation efficiency of the DNA machine decreases gradually than the single-molecular DNA nanomachine.

References

S1. Asanuma, H., Liang, X., Nishioka, H., Matsunaga, D., Liu, M., Komiyama, M., Nat. Protoc. 2007, 2, 203-212.

S2. Asanuma, H., Takarada, T., Yoshida, T., Tamaru, D., Liang, X., Komiyama, M., Angew. Chem. Int. Ed. 2001, 40, 2671-2673.

S3. Handley, D. A., 1989. Methods for synthesis of colloidal gold. In: Hayat, M. A. (Ed.) Colloidal Gold: Principles, Methods and Applications. Academic press, San Diego.

S4. H. Z. Kang, H. P. Liu, J. A. Phillips, Z. H. Cao, Y. Kim, Y. Chen, Z. Y. Yang, J. W. Li, W. H. Tan, Nano Lett. 2009, 9, 2690.